Optical properties of layered transition-metal halides



1990 J. Phys.: Condens. Matter 2 5439

(http://iopscience.iop.org/0953-8984/2/24/015)

J. Phys.: Condens. Matter 2 (1990) 5439–5453. Printed in the UK

# Optical properties of layered transition-metal halides

J Thomas†§, G Jezequel†§ and I Pollini‡§

† Laboratoire de Spectroscopie du Solide (Unité Associée No 1202 CNRS), Faculté des Sciences de l'Université de Rennes I, F35042 Rennes Cédex, France

‡ Dipartimento di Fisica, Università degli Studi di Milano, via Celoria 16, 20133 Milano, Italy

§ Laboratoire pour l'Utilisation du Rayonnement Electromagnétique, Université de Paris-Sud, 91405 Orsay Cédex, France

Received 2 October 1989, in final form 29 January 1990

**Abstract.** Near-normal incidence reflectance spectra of Fe, Co and Ni dihalides have been measured over the energy region 2–31 eV from 300 to 30 K with the use of synchrotron radiation. A complete study of the dielectric function $\hat{\varepsilon}(E)$, the energy-loss function $-\mathrm{Im}[1/\hat{\varepsilon}(E)]$, $\varepsilon_{0,\mathrm{eff}}(E)$ and $N_{\mathrm{eff}}(E)$ is made for all crystals by Kramers–Kronig analysis of the optical data. The structures observed up to about 13 eV in transition-metal chlorides and bromides have been assigned to allowed charge-transfer transitions, direct excitons and valence-to-conduction band transitions. Corners and maxima are then identified in terms of direct interband transitions at the symmetry points Γ, Z, F and L and along the symmetry line Λ of the Brillouin zone according to the available band structure of $FeCl_2$, $CoCl_2$, $NiCl_2$ and $NiBr_2$. The identified energy gap, due to $\Gamma_3^- \rightarrow \Gamma_1^+$ transitions at the zone centre, is found around 8.48 eV in $FeCl_2$, 8.54 eV in $CoCl_2$, 7.75 eV in $FeBr_2$ and 7.82 eV in $CoBr_2$. The saturation values of $\varepsilon_{0,\mathrm{eff}}(E)$ for chlorides ($\simeq$3) and bromides ($\simeq$4) point to a rather ionic character ($f_i = 0.7$–$0.8$) for all materials. Plasma resonance effects have been finally identified in the high-energy region, i.e. around 17–18 eV for the transition-metal chlorides and 16–17 eV for bromides.

## 1. Introduction

The fundamental electronic properties of ionic transition-metal halides (TMH) have been extensively studied lately in an attempt to elucidate their complicated electronic structure. Quite a number of works have been carried out in the ultraviolet region of the spectrum, ranging from optical studies [1–9] to photoemission measurements [10–15]. The large interband gaps (from p-like valence to s-like conduction bands) of the order of 6–9 eV of these crystals place their fundamental reflectance region in the vacuum-ultraviolet (VUV) portion of the spectrum, where the use of synchrotron radiation sources, providing an intense polarised continuum spectrum, is very promising [16]. In the past, most reflectance measurements [17–19] have been limited above 1050 Å (below 12 eV), where LiF windows and hydrogen discharge sources can be used. As a result, the measurements on $FeX_2$ [17], $NiX_2$ [18] and $CoX_2$ [19] (X = Cl, Br) only probe the lowest-energy portion of the fundamental absorption region. The optical properties of TMH are not only rich in structure, but also the origin of these features presents some challenging theoretical problems.

0953-8984/90/245439 + 15 $03.50 

Although a number of band-structure calculations [20] for transition-metal chlorides (TMC) and bromides (TMB) have been carried out, these alone cannot explain the observed spectra. Since the Coulomb interaction between electrons and holes, excited by the absorption of photons, is only weakly screened, strong exciton effects, as well as interband transitions, are present in the spectra. The effect of the exchange interactions on $\Gamma$ excitons in TMH has been discussed recently and the exchange splitting of the $\Gamma$ exciton states has been calculated in order to interpret the complicated fine structure observed [21]. Thus the problem of interpreting the electronic spectra is due not only to the difficulty of selecting the exciton peaks among those due to Van Hove singularities in the joint density of states, as occurs for instance in alkali halides or in partially ionic crystals, but also to the significant influence on the electronic properties arising from the presence of the unfilled, localised 3d shells of the transition-metal ions. Moreover, no theory that explains their optical, electrical and magnetic properties consistently has been established so far. Thus, the investigation of these materials is quite important.

The purpose of this work is to present new measurements at near-normal incidence reflectance of $FeCl_2$, $CoCl_2$, $FeBr_2$ and $CoBr_2$ in the photon energy range $2\,\text{eV} < \hbar\omega < 31\,\text{eV}$, for temperatures $30\,\text{K} < T < 300\,\text{K}$. The survey spectra of $NiCl_2$ and $NiBr_2$, which will also be reported here for the sake of completeness and comparison, have already been presented previously [5]. The dependence of the observed spectra on temperature, crystal structure and chemical composition is then used in the analysis of their electronic properties. Since the ultraviolet structure depends on both the crystal structure and atomic composition, we have discussed the present data by comparing the optical spectra of different crystals of TMC and TMB with very similar crystal structure and atomic composition. Finally, the interpretation is made in terms of the band structure of the materials, along the lines followed for nickel dihalides [5, 6] and transition-metal iodides (TMI) [7].

Transition-metal halides are ionic insulators [22] that crystallise in layer-like structures. The binding between the layers is of the van der Waals type, whereas in the plane of layers it is of ionic character. $FeCl_2$ and $CoCl_2$ have a crystal structure of the $CdCl_2$ type [23], space group $D_{3d}^5$; $FeBr_2$ and $CoBr_2$ crystallise in the $Cd(OH)_2$-type structure, space group $D_{3d}^3$. TMC and TMB usually crystallise as platelets perpendicular to the $c$ axis. The metal ions in all crystals have an octahedral coordination of chlorine and bromine ions, with a slight trigonal distortion.

In section 2 we briefly describe the method of determination of the reflectance power and dielectric function by application of the Kramers–Kronig (KK) dispersion analysis. In section 3 we present the reflectivity of Fe, Co and Ni dihalides, together with the results for real and imaginary parts of the dielectric function $\varepsilon_1(E)$ and $\varepsilon_2(E)$, as well as the energy-loss function, $-\text{Im}[1/\hat{\varepsilon}(E)]$, the effective dielectric constant $\varepsilon_{0,\text{eff}}(E)$ and the effective number $N_{\text{eff}}(E)$ of valence electrons per molecule contributing to the electronic process. Finally, in section 4 a general discussion of the optical results in terms of excitons, band-to-band transitions and plasmons is given.

## 2. Experimental techniques

Single crystals of $FeCl_2$, $FeBr_2$, $CoCl_2$ and $CoBr_2$ have been grown by means of a Bridgman-type gradient furnace [24]. Since all crystals are highly hygroscopic, the surface preparation has been made by stripping the samples in a glove-box filled with dry nitrogen and directly attached to the reflectometer. Synchrotron radiation from the

0.54 GeV storage ring ACO (Anneau de Collision d'Orsay) at the LURE (Orsay, France) was used as ultraviolet light source. The experimental apparatus is the same as that already employed in previous works [5, 7] and will not be described again. Instead, it is our wish to present in more detail the method we have used in order to determine the reflectance power and the dielectric function of our samples. Since TMC and TMB crystals are uniaxial (optical $c$ axis perpendicular to the planes of the layers) and the reflectance measurements are carried out with partially linearly polarised light, we have measured two sets of reflectance for a given incidence angle $\theta$, $R_1(\theta)$ or $R_2(\theta)$, corresponding mainly to either s or p polarisation [25–27]. The reflectometer used can rotate around the light beam axis, by exchanging the components s and p and thus measuring both $R_1(\theta)$ and $R_2(\theta)$. The results presented for the Fe and Co dihalides have been obtained by summing $R_1(\theta)$ and $R_2(\theta)$ with $\theta$ equal to 20° and 25°, and obtaining an average reflectance, whose value is very close to the one obtained for normal incidence ($\theta = 0$). The systematic error introduced by this approximation is less than 0.2%. In the case of Ni dihalides [5, 6] ($\theta < 20°$), instead, we have only measured $R_2(\theta)$ (mainly p component) with a consequent systematic error in the approximation used less than 2%. Thus, in general, the reflectance $R(E)$ or the dielectric functions $\varepsilon_1(E)$ and $\varepsilon_2(E)$ correspond to excitation with the electromagnetic field perpendicular to the $c$ axis. The KK relation

$$\alpha_1(\omega) = \frac{1}{\pi} \mathrm{P} \int_2^{31\,\mathrm{eV}} \ln \left| \frac{\omega' + \omega}{\omega' - \omega} \right| \frac{\mathrm{d} \lg[R(\omega')^{1/2}]}{\mathrm{d}\omega'} \mathrm{d}\omega'$$

is then applied to the spectra observed in the energy range 2–31 eV. However, the KK inversion relation only gives a partial phase shift $\alpha_1$ instead of the total phase shift $\alpha$, since the calculation of the shift would require the upper limit of integration to be equal to infinity ($\infty$) and the lower one equal to zero. A least-squares method [28] together with multi-angle reflectance data (between 20° and 70° in steps of 5° for the two polarisations used) allows the determination of the total phase shift $\alpha$ via the optical constants in a restricted energy range (for example, between 15 and 30 eV). The difference $\alpha - \alpha_1$ can then be determined in this interval and, by fitting these values with an interpolation formula of the type $A\omega + B\omega^3 + C\omega^5 + \ldots$ (corresponding to an expansion of $\lg[(\omega' + \omega)/(\omega' - \omega)]$ in power series) we finally obtain the necessary corrections over the whole spectral range. Furthermore, by assuming that $\alpha = 0$ in the low-energy range of transparency, one then gets the final result for $\alpha$, by using only a very small correction. Technical reports on the detailed optical method that we have employed for our experiments in both isotropic and uniaxial materials have recently been published [29].

## 3. Results

The room-temperature reflectance spectra of Fe and Co chlorides and bromides measured in the energy range 2–31 eV are shown in figures 1–4, together with the spectral dependence of the dielectric functions $\hat{\varepsilon}(E) = \varepsilon_1(E) + \mathrm{i}\varepsilon_2(E)$ and the energy-loss function $-\mathrm{Im}[1/\hat{\varepsilon}(E)]$, obtained by means of KK relations. We note that within each group of crystals (TMC and TMB) the spectra are rather similar in the energy range, specially beyond 7–8 eV, where there is a great resemblance as far as the position, lineshape and intensity of the peaks is concerned, as seen, for example, in the sequence of peaks labelled from D to L in figures 1–4. Further, the reflectance profile beyond 15 eV shows

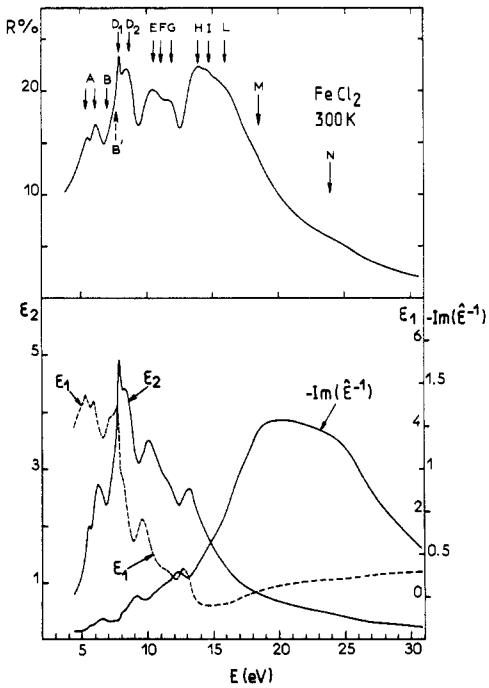


**Figure 1.** Spectral dependence of the reflectance $R$, the dielectric function $\hat{\varepsilon}(E) = \varepsilon_1(E) + i\varepsilon_2(E)$ and the energy-loss function $-\mathrm{Im}(1/\hat{\varepsilon})$ for $FeCl_2$ at room temperature.

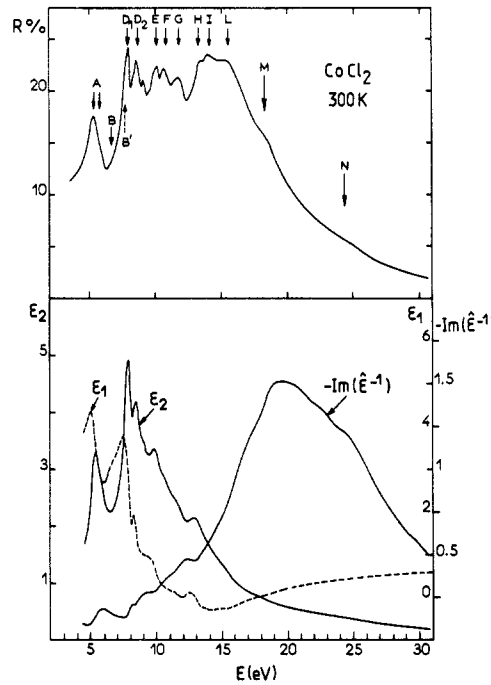


**Figure 2.** Spectral dependence of the reflectance $R$, the dielectric function $\hat{\varepsilon}(E) = \varepsilon_1(E) + i\varepsilon_2(E)$ and the energy-loss function $-\mathrm{Im}(1/\hat{\varepsilon})$ for $CoCl_2$ at room temperature.

a smooth decrease very much like that observed for ionic and covalent crystals. Figures 5 and 6 show detailed spectra of TMC and TMB at 300 and 30 K, respectively. That the spectra are very similar can be expected on account of the similar crystal structures and atomic constitution. Below 8 eV for TMC and 7 eV for TMB, we notice a shift to lower energy of the crystal structures A and B, when passing from Fe to Ni in chlorides and in bromides. As far as the energy positions of the low-energy structures are concerned, the present data on Fe and Co halides are in general agreement with the results of Martin *et al* [17] and Pollini [19] up to 11 eV. Also, a satisfactory agreement between the optical data of all the halides has been found with the film absorption made by Sakisaka *et al* [1] up to 8–9 eV; however, our present measurements on crystals show a better resolution in the whole energy range [30]. In the high-energy region, the optical energy-loss function, which describes the corresponding energy loss of fast electrons traversing the materials, presents broad bands between 15 and 25 eV, which do not appear to correspond directly to any observable structure in the spectra of $\varepsilon_2(E)$; and, besides, the values of the functions $\varepsilon_1(E)$ and $\varepsilon_2(E)$ are very small in the vicinity of the maximum of $-\mathrm{Im}[1/\hat{\varepsilon}(E)]$. For these reasons, we interpret the peaks of the energy-loss function as due to plasma resonances, whose energies can be calculated by means of Horie's relation [31], which gives the theoretical value of the plasmon energies in insulators. Energy electron-loss experiments have been carried out on Cr halides [8, 9], with a very nice agreement for the energy of the measured and optical plasmon energy. At the plasma frequency the oscillator strength corresponding to the valence band has been exhausted

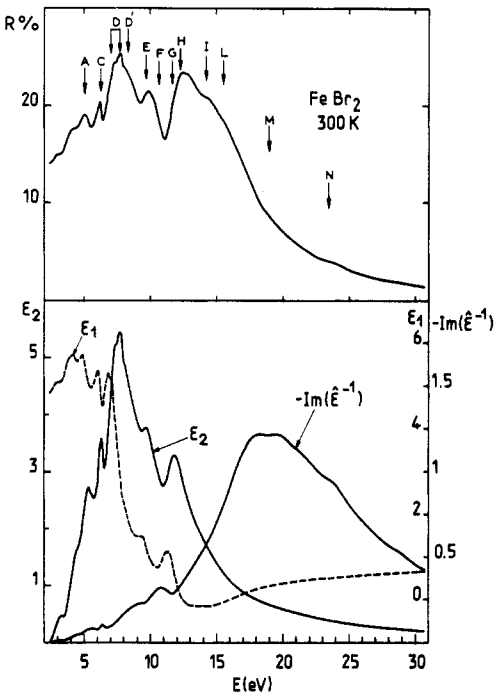


**Figure 3.** Spectral dependence of the reflectance $R$, the dielectric function $\hat{\varepsilon}(E) = \varepsilon_1(E) + i\varepsilon_2(E)$ and the energy-loss function $-\mathrm{Im}(1/\hat{\varepsilon})$ for $FeBr_2$ at room temperature.

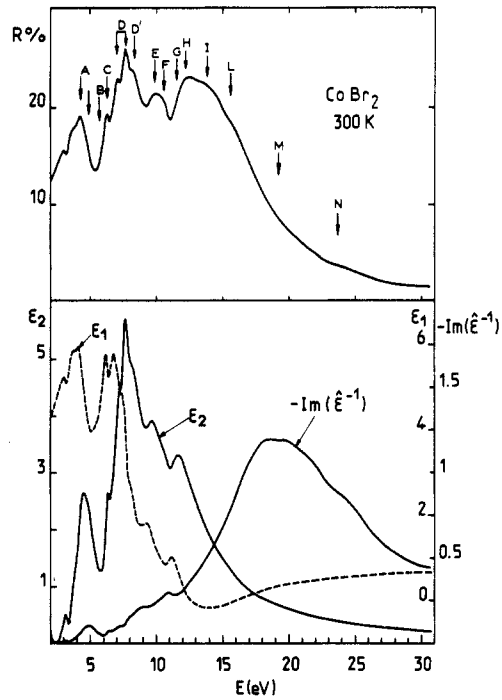


**Figure 4.** Spectral dependence of the reflectance $R$, the dielectric function $\hat{\varepsilon}(E) = \varepsilon_1(E) + i\varepsilon_2(E)$ and the energy-loss function $-\mathrm{Im}(1/\hat{\varepsilon})$ for $CoBr_2$ at room temperature.

and it can be assumed that $\varepsilon(\omega) = 1/(1 - \omega_p^2/\omega^2)$ in this region. About 12 electrons per molecule should contribute to $\hbar\omega_p$. There will also be strong damping of the plasma oscillations, since interband transitions occur at nearby energies. All the results obtained on plasmons in TMH, together with the available data of electron-beam energy-loss experiments reported by Best [32], have been summarised in table 1. It is worth while to compare the plasma energies of $CoCl_2$, $NiCl_2$ and $NiBr_2$ (listed in columns 2 and 5), since they give, in our opinion, the most meaningful theoretical and experimental values for plasmon energy (column 2). These are shifted to higher frequencies according to the

**Table 1.** Comparison of plasma frequencies (eV) as given by the free-electron value $(\hbar\omega_p)_{FE}$, the Horie relation $\hbar\omega_p$, the standard plasma dispersion relation $\varepsilon_1(\omega_p) = 0$, the maximum of the energy-loss function from optical data $-\mathrm{Im}(1/\hat{\varepsilon})_{max}$ and the electron energy loss.

| | $(\hbar\omega_p)_{FE}$ | $\hbar\omega_p$ | $\varepsilon_1(\omega_p) = 0$ | $-\mathrm{Im}(1/\hat{\varepsilon})_{max}$ | Energy loss |
|---|---|---|---|---|---|
| $FeCl_2$ | 16.0 | 18.1 | 17.0 | 20.0 | |
| $CoCl_2$ | 16.2 | 18.3 | 17.2 | 19.8 | 16.9 ± 0.2 |
| $NiCl_2$ | 16.3 | 18.4 | 16.7 | 20.2 | 18.0 ± 0.2 |
| $FeBr_2$ | 14.9 | 16.8 | 15.8 | 18.5 | |
| $CoBr_2$ | 15.2 | 17.1 | 16.0 | 19.2 | |
| $NiBr_2$ | 15.1 | 17.0 | 15.8 | 18.9 | 16.7 ± 0.2 |

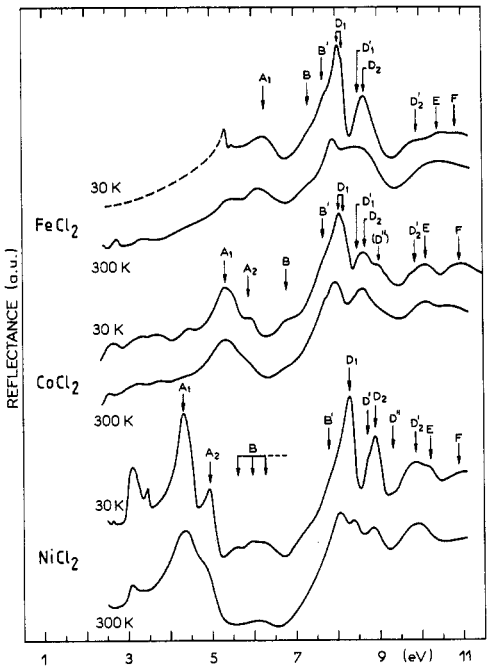


**Figure 5.** Details of the charge transfer (p → d) and exciton spectra of TMC in the region of the fundamental absorption threshold (p → s) at 300 and 30 K.

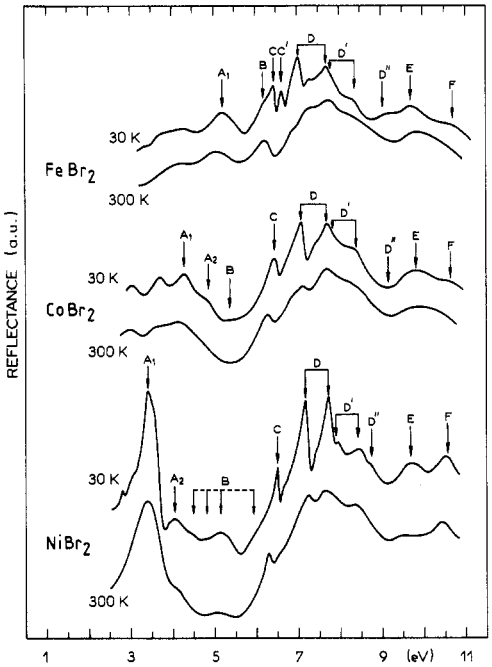


**Figure 6.** Details of the charge transfer (p → d) and exciton spectra of TMB in the region of the fundamental absorption threshold (p → s) at 300 and 30 K.

relation $(\hbar\omega_p)^2 = (\hbar\omega_p)^2_{FE} + E_g^2$, where $E_g$ is the fundamental forbidden gap and $(\hbar\omega_p)_{FE}$ is free-electron plasma energy, calculated from the relation $\omega_p^2 = 4\pi ne^2/m$, and seem more accurate than $(\hbar\omega_p)_{FE}$ (column 1). As for the experimental values of column 5, we note that they represent the most direct determination available of the plasma frequency. While we have found fairly good agreement for $NiCl_2$ and $NiBr_2$, it appears instead that the plasma energy of $CoCl_2$ (16.9 ± 0.2 eV) is lower than both the experimental (19.8 eV) and the theoretical (18.3 eV) values reported.

Figure 7 shows the spectral curves of the effective number of valence electrons participating in the absorption process, $N_{eff}(E)$, and the effective dielectric constant, $\varepsilon_{0,eff}$, calculated by means of conventional sum-rule relations [33]. We see that the curve of $N_{eff}(E)$ shows a change of slope around 8 eV and 7 eV for TMC and TMB, respectively. This fact should mark the onset of a new kind of electronic transition, which we interpret as a direct interband transition, in close analogy to the case of Ni halides [5, 6]. We also see that $N_{eff}(E)$ increases up to values between 13 and 16 effective electrons around 30 eV, beyond the maxima of the optical energy-loss functions (see figures 1–4). As for the spectral behaviour of the effective dielectric function, we find that the saturation values of all compounds are reached beyond 20 eV. This indicates the energy range of photons where no more contributions to $\varepsilon_{eff}(E)$ from deep valence states occur. Since this and other fine points related to the properties of the high-frequency dielectric functions for Fe, Co and Ni dihalides have been properly discussed in a previous paper [33] in connection with the predictions of the shell model, we shall not comment on them any further.

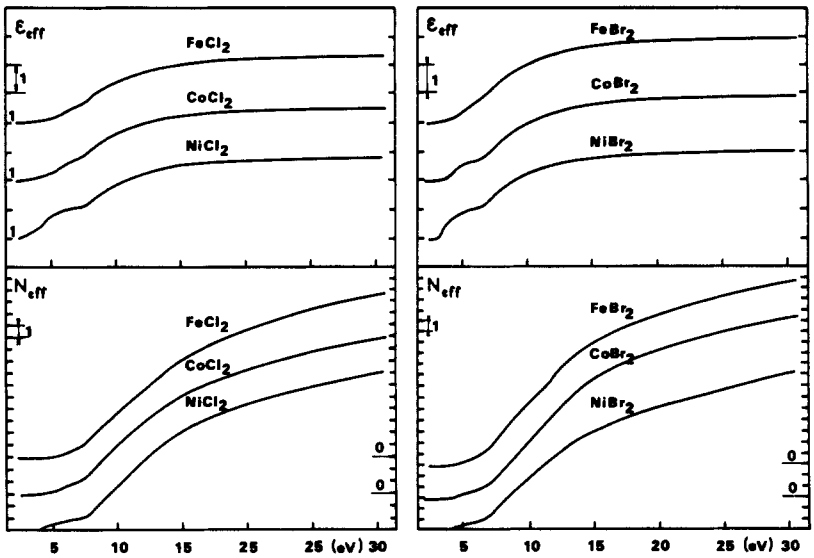


**Figure 7.** Effective dielectric constant $\varepsilon_{eff}(E)$ and effective number of electrons $N_{eff}(E)$ for TMH.

## 4. Discussion

The general features of the fundamental reflectance beyond 7–9 eV for TMC and TMB do not change practically, as the transition metal changes. The spectral profile in this high-energy region is only slightly different between chloride spectra (see figures 1 and 2) and bromide spectra (see figures 3 and 4), as can be easily observed either from reflectance spectra or from the dielectric functions $\varepsilon(E)$ over 8 eV. As remarked, this is expected on the grounds of the similar electronic structures of the compounds, which are very alike for the group of TMC and TMB: i.e. they show a valence band of the same character, owing to the same halogen ion, and almost the same kind of conduction band, mainly coming from the atomic 4s and 4p levels of the transition-metal ion. The main difference among the family members comes from the presence of a different number of 3d electrons, when passing from Fe($3d^6$; $e_g^2t_{2g}^4$) to Ni($3d^8$; $e_g^2t_{2g}^6$). Thus, the absorption profile beyond 8 eV should be attributed to a common excitation mechanism and should be determined essentially by valence-to-conduction band transitions. This excitation mechanism also occurs in alkali halides and, on the grounds of similar dielectric properties and ionicity, one would expect to observe strong excitonic effects, near the fundamental absorption edge. The peaks $D_1$ and $D_2$, shown in figure 5 for TMC, and the peaks D, shown in figure 6 for TMB, which present typical changes with temperature, are likely candidates for excitonic transitions. Moreover, one sees that the splitting of $D_1$ peaks in TMC (about 0.1 eV) and of D peaks in TMB (about 0.4–0.6 eV) have almost the same value of the spin–orbit splitting foreseen for excitons [34, 35] and found for instance in alkali halides [36]. The existence of small shoulders (reflecting Van Hove critical-point transitions, most often of $M_0$ and $M_1$ types) in proximity of strong excitonic peaks are then interpreted as evidence of critical point interband transitions. We think that the shoulders observed in the reflectance spectra at 30 K for TMH (see figures 5 and

6) just correspond to band-to-band transitions, whose labelling is to be done after consideration of the known band-structure calculations [20]. Here, we shall only discuss the cases of $FeCl_2$ and $CoCl_2$, following the detailed study made on nickel halides [5]. It is likely that most of the considerations can be extended to $FeBr_2$ and $CoBr_2$, for which band calculations are still lacking.

We shall now discuss the fundamental absorption edge for TMH and compare our present results with the available VUV data in order to clarify the overall phenomenological picture. It is well known that simple models based on electron transfer [37, 38] and atomic excitation [39] are often useful to explain the size of the optical gap in ionic compounds. In the 'charge-transfer' model the electronic transition energy around the fundamental gap is estimated by considering various parameters such as the anion electronic polarisation $\varphi$, the Madelung constant $\alpha$ and the cation–anion distance $r$, by the equation

$$\hbar\omega = [(2\alpha - 1)/r]e^2 + E - I - \varphi \tag{1}$$

where $\hbar\omega$ is the photon energy of the absorption process. If one considers only the change of the various parameters when passing from chlorides to bromides with the same transition-metal ion and that the crystal structures are quite similar ($\alpha$ and $r$ have almost the same values and $I$ is constant), one then gets that $\hbar\omega$ should vary with the same law as $E - \varphi$. Owing to the fact that $E$ decreases from 3.6 eV to 3.3 eV and $\varphi$ increases from 2.97 eV to 4.17 eV, on changing Cl by Br ions (passing for example $FeCl_2$ to $FeBr_2$), we find that the shifting of the optical gaps observed in the optical spectra (see for example figures 5 and 6) is roughly accounted for by equation (1). In particular, the experimental shifts are as follows: for Fe halides, 0.75 eV; for Co halides, 0.72 eV; and for Ni halides, 0.83 eV (see tables 2 and 3).

A different way to reach the same results is given by applying the dielectric theory (DT) to TMH. In this model Phillips and van Vechten [39] have defined the average separation ($E_g^{DT}$) of the valence and conduction bands as a sum of an ionic part $C$ and covalent part $E_h$ by

$$(E_g^{DT})^2 = C^2 + E_h^2 \tag{2}$$

with

$$E_h = ad^{-2.5} \tag{3}$$

and

$$C = b|Z_A/r_A - Z_B/r_B| \exp[-k_s(r_A + r_B)/2] \tag{4}$$

where $d$ is the nearest-neighbour distance (anion–cation); $Z_A$ and $Z_B$ are the valence numbers of elements A and B; $r_A$ and $r_B$ are their atomic radii; and $K_s$ is the Thomas–Fermi screening parameter. Using these relations with $a = 40.5$ and $b = 1.5$ we obtain for TMC, $E_g^{DT} = 8.32$ eV ($FeCl_2$), 8.31 eV ($CoCl_2$) and 8.39 eV ($NiCl_2$), and for TMB, $E_g^{DT} = 7.46$ eV ($FeBr_2$), 7.62 eV ($CoBr_2$) and 7.49 eV ($NiBr_2$). These results are in good agreement with the average experimental values for the forbidden energy gap of TMC and TMB, which is typically around 8.5–8.6 eV and 7.8 for chlorides and bromides, respectively [22]. In addition to this, we have also evaluated the ionicity for TMH, through its definition

$$f_i = C^2/(E_h^2 + C^2). \tag{5}$$

The results obtained, ranging from 0.79 ($FeCl_2$) to 0.74 ($NiBr_2$), indicate that these

**Table 2.** Electronic energies (eV) of experimental reflectance ($R$) structures (30 K) and of the imaginary part of the dielectric constant $\varepsilon_2$ for Fe, Co and Ni *chlorides*. The experimental values are compared with the theoretical ones (Theor.) on the grounds of the proposed assignments based on calculated band structures (Exc. denotes exciton).

| $FeCl_2$ | | | | $CoCl_2$ | | | | $NiCl_2$ | | | |
|---|---|---|---|---|---|---|---|---|---|---|---|
| Label | $R$ | $\varepsilon_2$ | Theor. | Label | $R$ | $\varepsilon_2$ | Theor. | Label | $R$ | $\varepsilon_2$ | Theor. |
| $A_1$ | 6.23 | 6.3 | Exc. $p \rightarrow d$ | $A_1$ | 5.35 | 5.4 | Exc. $p \rightarrow d$ | $A_1$ | 4.35 | 4.4 | Exc. $p \rightarrow d$ |
| | | | | $A_2$ | 5.90 | 5.9 | Exc. $p \rightarrow d$ | $A_2$ | 4.93 | 4.9 | Exc. $p \rightarrow d$ |
| B | 7.23 | 7.2 | $3p^6 \rightarrow 3p^5 3d^7$ | B | 6.85 | 6.8 | $3p^6 \rightarrow 3p^5 3d^8$ | B | 6.23 | 6.15 | $3p^6 \rightarrow 3p^5 3d^9$ |
| B′ | 7.66 | | | B′ | 7.7 | 7.7 | | B | 7.80 | | |
| $D_1$ | 8.01 | 7.92 | Exc. $\Gamma(\frac{3}{2})$ | $D_1$ | 8.10 | 7.98 | Exc. $\Gamma(\frac{3}{2})$ | $D_1$ | 8.30 | 8.07 | Exc. $\Gamma$ |
| $D_1$ | 8.10 | | Exc. $\Gamma(\frac{1}{2})$ | $D_1$ | 8.20 | | Exc. $\Gamma(\frac{1}{2})$ | | | | |
| $D_1'$ | 8.48 | | $\Gamma_3^- \rightarrow \Gamma_1^+$ : gap | $D_1'$ | 8.54 | | $\Gamma_3^- \rightarrow \Gamma_1^+$ : gap | $D_1'$ | 8.73 | 8.72 | $\Gamma_3^- \rightarrow \Gamma_1^+$ : gap |
| $D_2$ | 8.64 | 8.55 | Exc. Z | $D_2$ | 8.68 | 8.64 | Exc. Z | $D_2$ | 8.90 | 8.80 | Exc. Z |
| | | | | D″ | 9.04 | | | D″ | 9.30 | | |
| $D_2'$ | 9.68 | | $\Lambda$ line | $D_2'$ | 9.85 | | $\Lambda$ line | $D_2'$ | 9.9 | 9.8 | $\Lambda$ line |
| E | 10.3 | 10.1 | $Z_3^- \rightarrow Z_1^+$ : 10.3 | E | 10.1 | 9.9 | $Z_3^- \rightarrow Z_1^+$ : 10.2 | E | 10.2 | 10.1 | $Z_3^- \rightarrow Z_1^+$ : 10.3 |
| F | 10.9 | 10.8 | $F_2^- \rightarrow F_1^+$ : 10.8 | F | 10.8 | 10.7 | $F_2^- \rightarrow F_1^+$ : 10.8 | F | 10.9 | 10.8 | $F_2^- \rightarrow F_1^+$ : 10.7 |
| G | 11.9 | 11.7 | | G | 11.8 | 11.6 | | G | 11.9 | 11.8 | $L_2^- \rightarrow L_1^+$ : 11.7 |
| | | | | | | | | | | | $Z_3^+ \rightarrow Z_2^-$ : 12.1 |
| H | 13.9 | 13.2 | | H | 13.4 | 13.0 | | H | 13.3 | 13.1 | $\Gamma_3^+ \rightarrow \Gamma_2^-$ : 12.7 |
| | | | | | | | | | | | $L_1^+ \rightarrow L_2^-$ : 13.8 |
| I | 14.6 | | | I | 14.1 | 14.0 | | I | 14.3 | 13.7 | $F_1^+ \rightarrow F_2^-$ : 14.3 |
| | | | | | | | | | | | $F_2^- \rightarrow F_1^+$ : 14.4 |
| L | 15.9 | 15.8 | | L | 15.3 | 15.3 | | L | 15.4 | 15.0 | $\Gamma_3^- \rightarrow \Gamma_1^+$ : 15.2 |
| | | | | | | | | | | | $L_2^- \rightarrow L_1^+$ : 15.3 |
| M | 18.2 | 18.0 | | M | 18.3 | 18.1 | | M | 18.3 | 18.0 | $Z_1^+ \rightarrow Z_3^-$ : 17.3 |
| | | | | | | | | | | | $\Gamma_1^+ \rightarrow \Gamma_3^-$ : 18.2 |
| N | 23.8 | 23.8 | | N | 24.6 | 24.5 | | | | | |

**Table 3.** Electronic energies (eV) of experimental reflectance ($R$) structures (30 K) and of the imaginary part of the dielectric constant $\varepsilon_2$ for Fe, Co and Ni *bromides*. The experimental values are compared with the theoretical ones (Theor.) on the grounds of the proposed assignments based on calculated band structures (Exc. denotes exciton).

| $FeBr_2$ | | | | $CoBr_2$ | | | | $NiBr_2$ | | | |
|---|---|---|---|---|---|---|---|---|---|---|---|
| Label | $R$ | $\varepsilon_2$ | Theor. | Label | $R$ | $\varepsilon_2$ | Theor. | Label | $R$ | $\varepsilon_2$ | Theor. |
| $A_1$ | 5.20 | 5.28 | Exc. $p \rightarrow d$ | $A_1$ | 4.29 | 4.24 | Exc. $p \rightarrow d$ | $A_1$ | 3.42 | 3.50 | Exc. $p \rightarrow d$ |
| | | | | $A_2$ | 4.85 | 4.80 | Exc. $p \rightarrow d$ | $A_2$ | 4.05 | 4.15 | Exc. $p \rightarrow d$ |
| B | 6.17 | | $4p^6 \rightarrow 4p^5 3d^7$ | B | 5.37 | | $4p^6 \rightarrow 4p^5 3d^8$ | B | 5.15 | 5.05 | $4p^6 \rightarrow 4p^5 3d^9$ |
| C | 6.42 | 6.28 | Exc. | C | 6.45 | 6.30 | Exc. | C | 6.50 | 6.30 | Exc. |
| C′ | 6.61 | | | | | | | | | | |
| $D_1$ | 7.03 | 6.90 | Exc. $\Gamma(\frac{3}{2})$ | $D_1$ | 7.08 | 6.90 | Exc. $\Gamma(\frac{3}{2})$ | $D_1$ | 7.15 | 7.20 | Exc. $\Gamma(\frac{3}{2})$ |
| $D_2$ | 7.67 | 7.66 | Exc. $\Gamma(\frac{1}{2})$ | $D_2$ | 7.69 | 7.65 | Exc. $\Gamma(\frac{1}{2})$ | $D_2$ | 7.70 | 7.60 | Exc. $\Gamma(\frac{1}{2})$ |
| $D_1'$ | 7.75 | | $4p(\frac{3}{2}) \rightarrow 4s$ : gap | $D_1'$ | 7.82 | | $4p(\frac{3}{2}) \rightarrow 4s$ : gap | $D_1'$ | 7.90 | 7.80 | $(\frac{3}{2})\Gamma_3^- \rightarrow \Gamma_1^+$ : gap |
| $D_2'$ | 8.36 | 8.30 | $4p(\frac{1}{2}) \rightarrow 4s$ : gap | $D_2'$ | 8.39 | 8.3 | $4p(\frac{1}{2}) \rightarrow 4s$ : gap | $D_2'$ | 8.44 | 8.30 | $(\frac{1}{2})\Gamma_3^- \rightarrow \Gamma_1^+$ : gap |
| D″ | 9.03 | | | | | | | D″ | 8.74 | | |
| E | 9.70 | 9.65 | | E | 9.82 | 9.65 | | E | 9.69 | 9.40 | $Z_3^- \rightarrow Z_1^+$ : 9.4 |
| F | 10.67 | | | F | 10.63 | 10.4 | | F | 10.58 | 10.3 | $F_2^- \rightarrow F_1^+$ : 9.9 |
| | | | | | | | | | | | $L_2^- \rightarrow L_1^+$ : 10.8 |
| G | | 11.7 | | G | | 11.6 | | G | 11.7 | 11.5 | $F_1^+ \rightarrow F_2^-$ : 11.5 |
| | | | | | | | | | | | $L_2^- \rightarrow L_1^+$ : 11.8 |
| H | 12.3 | | | H | 12.2 | | | H | 12.6 | 12.4 | $\Gamma_3^+ \rightarrow \Gamma_2^-$ : 11.9 |
| | | | | | | | | | | | $L_1^+ \rightarrow L_2^-$ : 13.0 |
| I | 14.2 | | | I | 13.8 | | | I | 13.9 | 13.6 | $F_1^+ \rightarrow F_2^-$ : 13.5 |
| | | | | | | | | | | | $F_2^- \rightarrow F_1^+$ : 13.6 |
| L | 15.5 | | | L | 15.6 | | | L | 15.1 | 14.9 | $F_2^- \rightarrow F_1^+$ : 15.0 |
| | | | | | | | | | | | $L_1^+ \rightarrow L_2^-$ : 15.2 |
| M | 19.0 | | | M | 19.2 | | | M | 16.8 | 16.5 | $Z_1^+ \rightarrow Z_3^-$ : 16.5 |
| N | 23.5 | | | N | 23.6 | | | | | | |

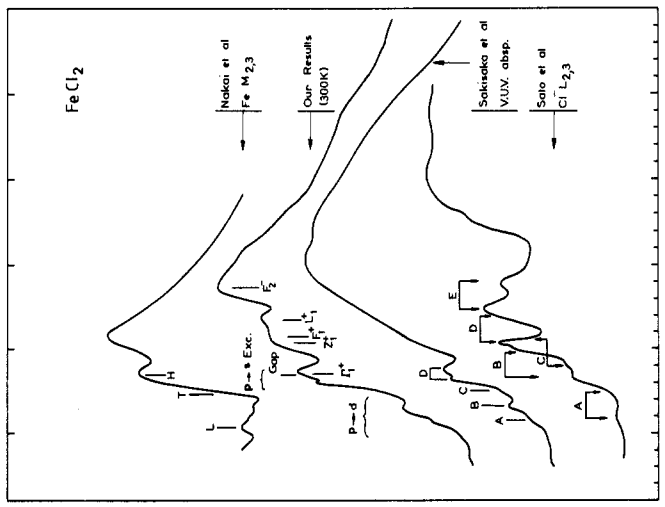


**Figure 8.** Review of VUV results obtained by different researchers on $FeCl_2$: $M_{2,3}$ absorption spectrum by Nakai *et al* [10]; absorption coefficient (this work); film absorption spectrum by Sakisaka *et al* [1]; and $Cl^-$ $L_{2,3}$ absorption spectrum by Sato *et al* [3].

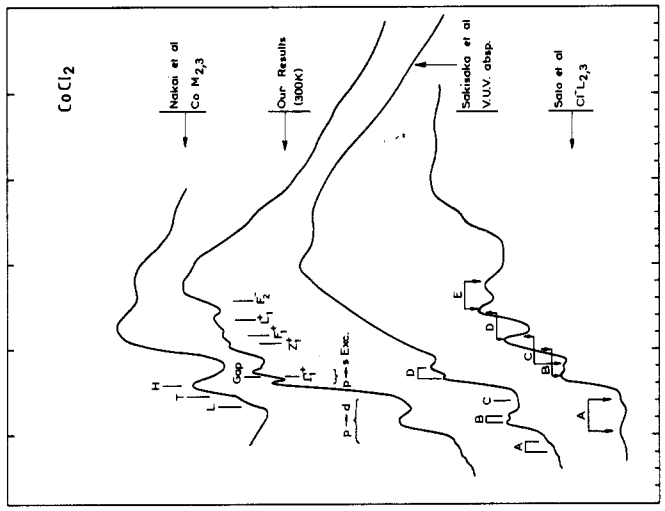


**Figure 9.** Review of VUV results obtained by different researchers on $CoCl_2$. Same references as in figure 8.

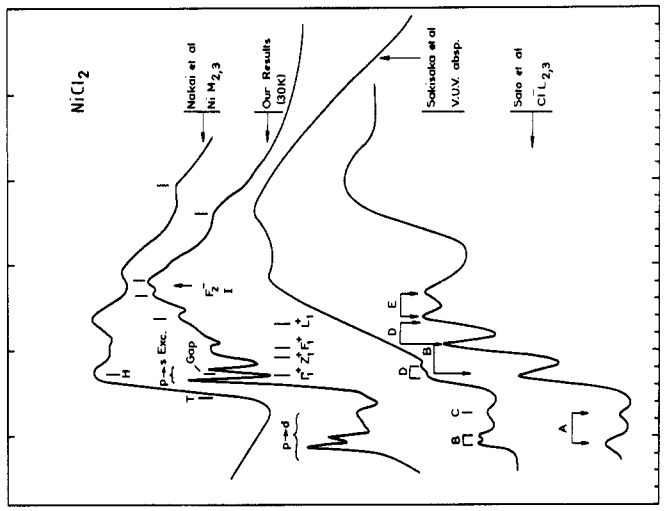


**Figure 10.** Review of VUV results obtained by different researchers on $NiCl_2$. Same references as in figure 8.

halides are rather ionic in character, only slightly less than the alkali halides. In a previous paper [22], besides having reported the ionicity figures for a number of TMH, we have also discussed the applicability of the DT to TMH and compared the results obtained by considering different ionicity scales.

In figures 8–10 we have shown a comparison among different spectra measured on $FeCl_2$, $CoCl_2$ and $NiCl_2$ with various experimental techniques. The abscissae of the ultraviolet spectra and soft x-ray absorption spectra are placed so that a close correspondence between the absorption thresholds observed in the spectra measured on the same crystal is obtained. We note that the structures of $FeCl_2$, $CoCl_2$ and $NiCl_2$ can be divided into two groups, which are separated by a strong absorption edge around 8–9 eV. At lower energy one finds a group of weaker bands between 4 and 7 eV, and beyond the threshold (T line), the main structures of the spectra rise up to the intense and broad bands observed between 15 and 20 eV. Looking for correspondence among the peaks of the different spectra, one must remember that the joint density of states for the soft x-ray absorption process is actually the density of states of the conduction band. Thus, the absorption profiles due to different core levels are likely to be similar, since they all reflect the spectrum of the density of states of the conduction band. Although the $M_{2,3}$ spectra of Fe, Co and Ni chlorides cannot be compared too well with fundamental VUV absorption spectra because of different starting levels (3p of transition metal in $M_{2,3}$ spectra and 3p of chlorine in VUV spectra), nevertheless two groups of peaks with some correspondence in the spectra shown may be found. Fe, Co and Ni ions have unpaired electrons in the 3d shell and the $M_{2,3}$ absorption is due to the transition from the 3p levels of these metal ions. Therefore, the influence of the 3d states will affect the $M_{2,3}$ spectra, which show an absorption profile similar to that of charge-transfer processes in VUV spectra. It is also reasonable to make a correspondence between the peak H in $M_{2,3}$ spectra of Fe, Co and Ni chlorides and the exciton-dominated interband structure around 9–10 eV of the VUV absorption spectra due to transitions associated to the bottom of the conduction bands $\Gamma_1^+$ or to the doublet D of the absorption spectrum reported by Sakisaka *et al* [1]. The same result is found by considering the $Cl^-$ $L_{2,3}$ spectra [2], whose interpretation is, however, complicated by peak doubling due to core-level spin–orbit splitting. It seems reasonable, however, to attribute the doublet A to charge-transfer transitions $p \rightarrow d$ on the low-energy side of the absorption edge, as originally proposed by Sato *et al* [3], and the doublet B, beyond that threshold, to excitons connected with the point $\Gamma_1^+$ of the conduction band in our spectra. Then the doublets D and E may be ascribed to direct interband transitions connected with critical points $Z_1^+$, $F_1^+$ and $L_1^+$. Owing to the overall similarity of the spectra presented and, by considering the behaviour with temperature of TMC (see figure 5), where the great modification of the structures designated as $p \rightarrow s$ excitons is apparent, we can confirm the interpretation originally given by Sato *et al* concerning the charge-transfer process to d states and our foregoing interpretation on interband excitons [8–10]. In particular, looking at the spectra reviewed in figures 9 and 10, we can evaluate the average energy separation of the localised d states from the bottom of the conduction bands, which in the case of TMC is about 4–5 eV.

In the following, we shall refer to the band structure of $FeCl_2$ and $CoCl_2$, which are reproduced in figures 11 and 12. We note that the ordering and relative positions of the valence and conduction band states for $FeCl_2$ and $CoCl_2$ are very similar to those calculated for $NiCl_2$ [5]. Here, we will only discuss the case of TMC, for which there is more theoretical support, and then we shall make some considerations on TMB on account of the very similar optical data and supposedly similar electronic structure. To

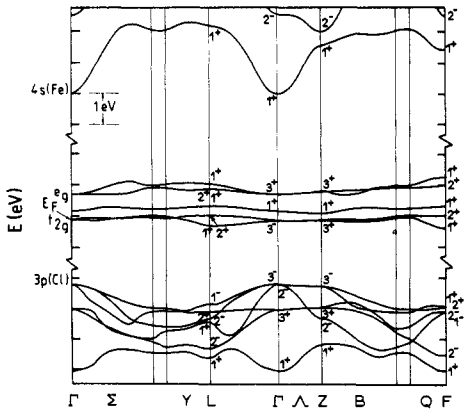


**Figure 11.** Self-consistent band structure of $FeCl_2$ determined by the intersecting-sphere model according to Antoci and Mihich [20]. The forbidden gap has been rigidly shifted in order to reach agreement between the optical gap considered at the zone centre (Γ). The Fermi level ($E_F$) has been also reported.

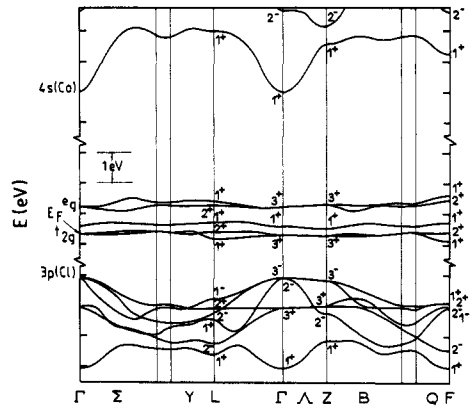


**Figure 12.** Self-consistent band structure of $CoCl_2$ determined by the intersecting-sphere model according to Antoci and Mihich [20]. The forbidden gap has been rigidly shifted in order to reach agreement between the optical gap considered at the zone centre (Γ). The Fermi level ($E_F$) has been also reported.

this end, we have summarised in tables 2 and 3 all the experimental results and the assignments proposed after consideration of the optically allowed transitions, starting from the uppermost valence bands to the conduction bands labelled by means of their irreducible representations ($1^+, 2^-, 3^+, \ldots$) at the high-symmetry points of the Brillouin zone.

The fact that band structures of TMC and TMB are very similar to the measured optical spectra provides some help in making reasonably safe attributions in a region where the interpretation of the ultraviolet spectra is necessarily difficult since several electronic transitions are possible at the same time and the spectra show broad band structures. In fact, since no joint density of states was calculated, we can only suggest the most likely assignments for some interband transitions beyond the fundamental gaps, which are observed around 8.60 eV for TMC and 7.80 eV for TMB (D′ structures).

Interband transitions begin at 8.48 eV in $FeCl_2$ and at 8.54 eV in $CoCl_2$ with an $M_0$-type critical point, produced by the $\Gamma_3^- \rightarrow \Gamma_1^+$ transition. In the reflectance spectra, shown in figure 5, we see that the fundamental gap, denoted by $D_1'$ in $FeCl_2$ and $CoCl_2$ and by D′ in $NiCl_2$, is between excitons Γ and Z. The exciton peaks are rather large and weaken the interband transitions; in $FeCl_2$ and $CoCl_2$, besides, the first exciton is also slightly doubled because of the effect of the spin–orbit interaction (0.1 eV) of the chlorine ions. The following interband transitions take place along the symmetry line and at the Z point. We assign the $D_2'$ peak at 9.68 eV in $FeCl_2$ and 9.85 eV in $CoCl_2$, and the peak E at 10.3 eV in $FeCl_2$ and 10.1 eV in $CoCl_2$ to these transitions (see figures 1, 2 and 5). The next band-to-band transition arises at the F point, that is, the $F_2^- \rightarrow F_1^+$: 10.9 eV in $FeCl_2$ and 10.8 eV in $CoCl_2$. We assign the peak F to that transition. We then see in tables 2 and 3 that the energies of the band-to-band transitions at Γ, F, Z and L cover the energy region between 11 and 14 eV. Thus, these transitions, listed in table 2, may be assigned to peaks G, H and I of $FeCl_2$ and $CoCl_2$. These assignments, which agree reasonably well with the calculated band structure (theoretical values in column 4 of table 2) and with those reported for Ni halides, are given in tables 2 and 3, where the

examples of $FeCl_2$ and $CoCl_2$ are compared with that of $NiCl_2$ and those of $FeBr_2$ and $CoBr_2$ with that of $NiBr_2$.

## 5. Conclusions

The optical spectra of transition-metal halides have been divided into charge-transfer, interband scattering and excitonic structures. The similarity between the spectra suggests that their interpretation can be attempted on the basis of a self-consistent band structure of transition-metal chlorides and $NiBr_2$, provided that the band-gap value is empirically adjusted. On this basis, nearly all the main spectral features below 12 eV can be identified with the suggested excitation mechanisms. The exciton structure, which contains sharp peaks overlapping the scattering continuum, is assigned, and the correct order of magnitude for the binding energy is found. Along these lines, it appears that the peaks below the threshold of TMH should be assigned to charge-transfer transitions from the p-type valence band to quasi-localised $3d^n$ states, while those occurring just above the threshold are assigned to direct electronic transitions between the halogen p levels and the metal s levels. Plasma resonance effects occur in all materials and are suggested by the function $-\mathrm{Im}[1/\hat{\varepsilon}(E)]$, which presents broad and intense maxima in the region 18–20 eV.

## Acknowledgments

The authors thank the technical staff of the 'Laboratoire d'Utilisation du Rayonnement Electromagnétique', as well as the members of the 'Laboratoire de l'Accélerateur Linéaire' (Orsay) for providing the ACO beam during the course of the experiments. They are also grateful to S Legrand of the Centre d'Etudes Nucléaires de Saclay (Gif-sur-Yvette, France) for providing single crystals of Fe and Co dichlorides and dibrodimes. The manuscript was prepared in part while one of us (IP) was visiting the University of Rennes in the framework of the scientific cooperation agreement between the 'Centre Nationale de la Recherche Scientifique' and the 'Consiglio Nazionale delle Ricerche'.

## References

[1] Sakisaka Y, Ishii T and Sagawa T 1974 *J. Phys. Soc. Japan* **36** 1365, 1372
[2] Sakisaka Y 1975 *J. Phys. Soc. Japan* **38** 505
[3] Sato S, Ishii T, Nagakura I, Aita O, Nakai S, Yokota M, Ichikawa K, Matsuoka G, Kono S and Sagawa T 1971 *J. Phys. Soc. Japan* **30** 459
[4] Shin S, Suga S, Taniguchi M, Kanzaki H, Shibuya S and Yamaguchi T 1982 *J. Phys. Soc. Japan* **51** 906
[5] Pollini I, Thomas J, Jezequel G, Lemonnier J C and Mamy R 1983 *Phys. Rev.* B **27** 1303
[6] Pollini I, Thomas J, Jezequel G, Lemonnier J C and Lenselink A 1984 *Phys. Rev.* B **29** 4716
[7] Pollini I, Thomas J and Lenselink A 1984 *Phys. Rev.* B **30** 2140
[8] Carricaburu B, Ferre J, Mamy R, Pollini I and Thomas J 1986 *J. Phys. C: Solid State Phys.* **19** 4985
[9] Pollini I, Thomas J, Carricaburu B and Mamy R 1990 *J. Phys.: Condens. Matter* **1** 7695
[10] Nakai S, Nakamori H, Tomita A, Tsutsumi K, Nakamura N and Sugiura C 1974 *Phys. Rev.* B **9** 1870
[11] Hufner S and Wertheim G K 1973 *Phys. Rev.* B **8** 4857
[12] Hufner S 1984 *Solid State Commun.* **49** 1177; 1985 *Solid State Commun.* **53** 707
[13] Ishii T, Kono S, Suzuki S, Nagakura I, Sagawa T, Kato R, Watanabe M and Sato S 1975 *Phys. Rev.* B **12** 4320
[14] Kakisaki A, Sugano K, Ishii T, Sugawara H, Nagakura I and Shin S 1983 *Phys. Rev.* B **28** 1026

[15] Starnberg H I, Johnson M T and Hughes H P 1986 *J. Phys. C: Solid State Phys.* **19** 2689
[16] Godwin R P 1969 *Springer Tracts Mod. Phys.* **51** 1
[17] Martin L, Couget A and Pradal F 1971 *C.R. Acad. Sci. Paris* **273** 873
[18] Pollini I and Spinolo G 1974 *J. Phys. C: Solid State Phys.* **7** 2391
[19] Pollini I 1977 *Phys. Status Solidi* b **79** 231
[20] Antoci S and Mihich L 1978 *Phys. Rev.* B **18** 5768; 1980 *Phys. Rev.* B **21** 3383
[21] Folkert W and Haas C 1985 *Phys. Rev.* B **32** 2559
[22] Thomas J and Pollini I 1985 *Phys. Rev.* B **32** 2522
[23] Wycoff R W G 1963 *Crystal Structures* vol 1 (New York: Interscience)
[24] Legrand S 1976 *J. Crystal Growth* **35** 208
[25] Lemmonnier J C, Thomas J and Robin S 1973 *J. Phys. C: Solid State Phys.* **6** 3205
[26] Uzan E 1968 *Opt. Acta* **15** 237
[27] Thomas J, Lemonnier J C and Robin S 1972 *Opt. Acta* **19** 983
[28] Jezequel G, Lemonnier J C and Thomas J 1977 *J. Phys. F: Met. Phys.* **7** 1613
[29] Thomas J, Jezequel G and Pollini I 1988 *J. Opt. Soc. Am.* **5** 344; 1989 *J. Opt. Soc. Am.* **6** 27
[30] Ishii T 1985 *Technical Report of ISSP* 1523, 1, Institute for Solid State Physics
[31] Horie C 1959 *Prog. Theor. Phys.* **21** 113
[32] Best P E 1962 *Proc. Phys. Soc. Lond.* **80** 1308
[33] Pollini I, Benedek G and Thomas J 1984 *Phys. Rev.* B **29** 3617
[34] Knox R S and Inchauspe N 1959 *Phys. Rev.* **116** 1093
[35] Eby J E, Teegarden K and Dutton D B 1959 *Phys. Rev.* **116** 1099
[36] Mott N F and Gurney R W 1940 *Electronic Processes in Ionic Crystals* (London: Oxford University Press) ch 3
[37] Nikitine S 1960 *Exciton Spectra in Semiconductors and Ionic Compounds* (Strasbourg: University Press)
[38] Knox R S 1963 *Theory of Excitons, Solid State Physics* (New York: Academic) Suppl. 5
[39] Phillips J C and van Vechten J A 1969 *Phys. Rev. Lett.* **22** 705